Supplmetal information: Electronic structures of Bi_2Se_3 and $Ag_xBi_2Se_3$ under pressure probed by high-resolution x-ray absorption spectroscopy

Hitoshi Yamaoka (山岡人志),[1] Harald O. Jeschke,[2] Xiaofan Yang,[2] Tong He,[2] Hidenori Goto (後藤秀徳),[2] Nozomu Hiraoka (平岡 望),[3] Hirofumi Ishii (石井啓文),[3] Jun'ichiro Mizuki (水木純一郎),[4] and Yoshihiro Kubozono (久保園芳博)[2]

[1] *RIKEN SPring-8 Center, Sayo, Hyogo 679-5148, Japan*
[2] *Research Institute for Interdisciplinary Science, Okayama University, Okayama 700-8530, Japan*
[3] *National Synchrotron Radiation Research Center, Hsinchu 30076, Taiwan*
[4] *Graduate School of Science and Technology, Kwansei Gakuin University, Sanda, Hyogo 669-1337, Japan*

A. Details of the analyses of the PFY-XAS spectra

Figures S1(a) and S1(b) show fit examples of the PFY-XAS spectra (the same figures as Fig. 2 in the main text). Normally the absorption spectra consist of the Raman part near the absorption edge, the part of the EXAFS structure above the edge with many peaks, and the fluorescence part of an arctan-like background. We used a Voigt function for each peak in the fits. The spectra are normalized by the intensities. The pressure-induced change in the spectra is not large and we can deduce small relative change in the spectra by changing the data at a given pressure to the data of next pressure.

In Fig. S1(a) the peak A has an asymmetric profile and we assumed a main large peak with an additional small peak. In this case the energy of the peak A is calculated as a mean value of tow peaks taking into account the weight of each peak intensity. In Fig. S1(b) a weak peak D is observed near the absorption edge. This peak corresponds to the Bi 6*s* band. The change in the peak D is important because it locates near the Fermi level. High-resolution spectroscopy makes it possible to separate the peak D to other peaks.

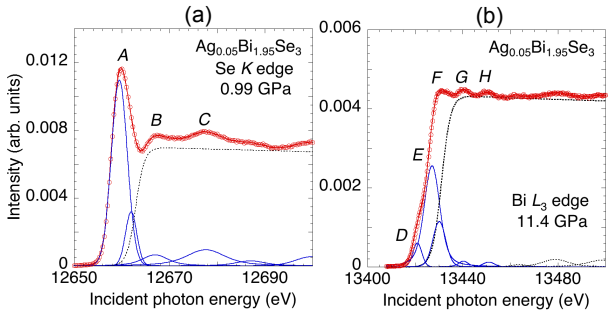

FIG. S1. (Color online). (a) A fit example of the PFY-XAS spectra of $Ag_{0.05}Bi_{1.95}Se_3$ at the Se-K absorption edge and at 0.99 GPa. Main peaks around the absorption edge are labeled as A, B, and C. (b) A fit example of the PFY-XAS spectra of $Ag_{0.05}Bi_{1.95}Se_3$ at the Bi-L_3 absorption edge and at 11.4 GPa. Main peaks around the absorption edge are labeled as D, E, F, G, and H. (The same figures as Fig. 2 in the main text.)

B. Pressure dependence of the PFY-XAS spectra of $Sr_{0.09}Bi_2Se_{3.61}$

Figures S2(a) and S2(f) show the pressure dependence of the PFY-XAS spectra of $Sr_{0.19}Bi_2Se_3$ at the Se-K and Bi-L_3 absorption edges. Key differences of the pressure dependence of the electronic structure of $Sr_{0.19}Bi_2Se_3$ compared to those of Bi_2Se_3 and $Ag_{0.05}Bi_{1.95}Se_3$ are a sudden change in the electronic structure around 2-3 GPa and a weak intensity of the peak D component. Note that the phase diagram of the superconductivity in Fig. S2(c) and S2(h) are for $Sr_{0.065}Bi_2Se_3$. [1] Highly doped samples of $Sr_{0.15}Bi_2Se_3$ [2] and $Sr_{0.1}Bi_2Se_3$ [3] also showed a rapid decrease of T_c at low pressures. In $Sr_{0.1}Bi_2Se_3$, no reentrant superconducting phase was observed up to 8 GPa. [3] Here, we also study the highly doped sample of $Sr_{0.19}Bi_2Se_3$ and T_c of the present sample has not been measured. However, we could believe that a larger content of Sr more than 5% induces the superconductivity with larger superconducting volume fraction. [4–6] In this case, it has been considered that Sr atoms may be mainly inserted between Bi and inner Se layers. [5]

In $Sr_{0.19}Bi_2Se_3$, the intensity of the peak A (Se 4p band) of the PFY-XAS spectra at the Se-K absorption edge in Fig. S2(d) decreased up to 2.5 GPa, suddenly increased at pressures between 2.5 and 3.5 GPa, and did not change much with further increase of the pressure up to 28.3 GPa. The energies of the absorption edge in Fig. S2(c) and the peak A in Fig. S2(d) followed the pressure-induced change in the intensity of the peak A, however, there was an anomaly at 16.4 and 19.4 GPa. The change in the intensity of the peak A up to 16 GPa and the increase of its intensity around 15-16 GPa seems to closely correlate to the pressure dependence of T_c although we do not understand the decrease of the intensity of peak A above 20 GPa at present.

In $Sr_{0.19}Bi_2Se_3$, the peak D (Bi 6s band) in Fig. S2(i) is not as clearly observed as a shoulder peak as in Bi_2Se_3 and $Ag_{0.05}Bi_{1.95}Se_3$. The peak D of $Sr_{0.5}Bi_2Se_3$ was observed clearly as shown in Fig. 1(c) in the main text and thus the large Sr doping makes the empty Bi 6s states small. The intensities of the peak D and E (6d t_{2g} band) increased and decreased rapidly at 2.5 GPa, respectively, as shown in Figs. S2(i) and S2(j) and shows little change

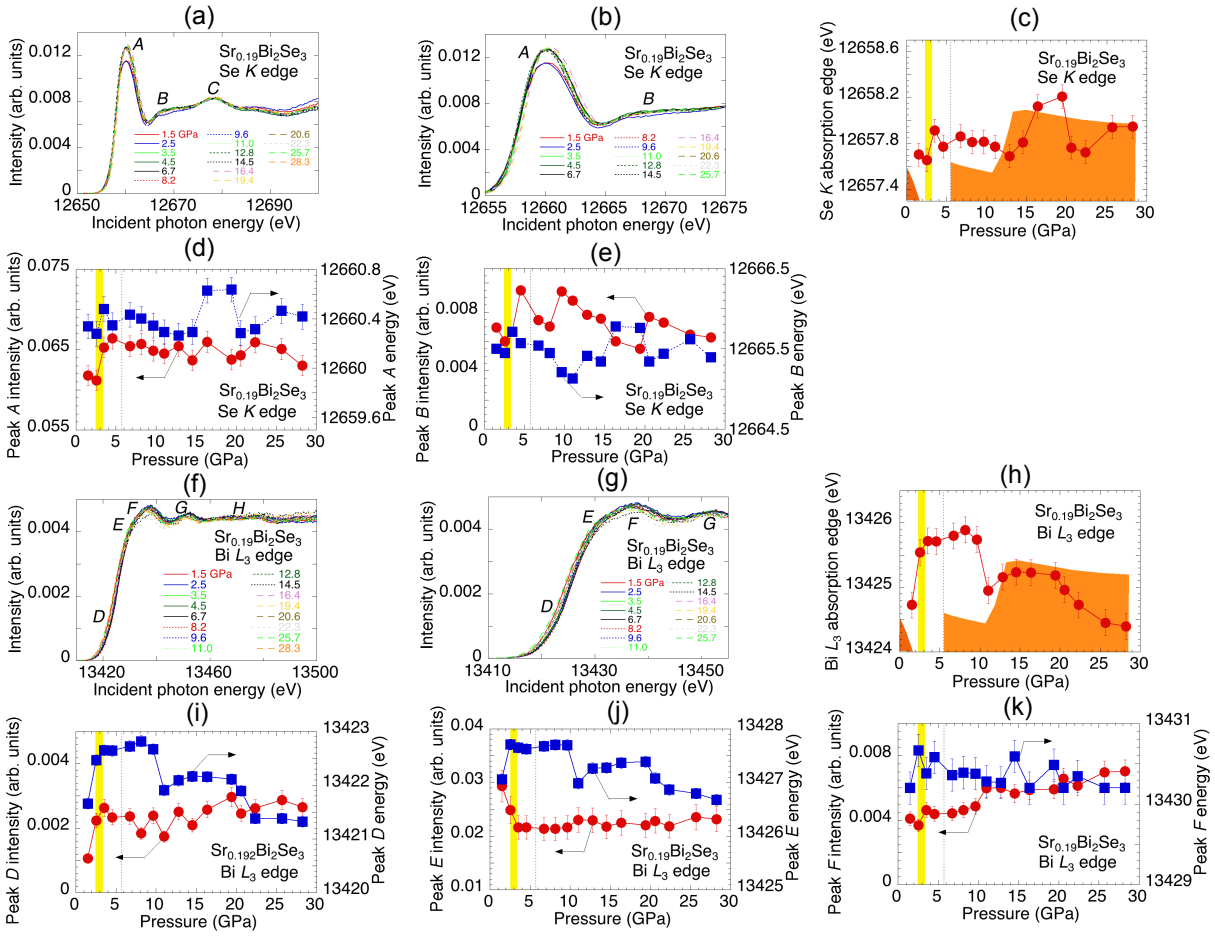

FIG. S2. (Color online). (a) Pressure dependence of the PFY-XAS spectra of $Sr_{0.19}Bi_2Se_3$ at the Se-K absorption edge. (b) Expanded views of the PFY-XAS spectra in (a) around the Se-K absorption edge. (c) Pressure dependence of the energy of the Se-K absorption edge. (d) & (e) Pressure dependence of the intensity and energy of the peaks A and B of the PFY-XAS spectra at the Se-K absorption edge, respectively. (f) Pressure dependence of the PFY-XAS spectra of $Sr_{0.19}Bi_2Se_3$ at the Bi-L_3 absorption edge. (g) Expanded views of the PFY-XAS spectra in (f) around the Se K-absorption edge. (h) Pressure dependence of the energy of the Bi-L_3 absorption edge. (i), (j), & (k) Pressure dependence of the intensity and energy of the peaks D, E, and F of the PFY-XAS spectra at the Bi-L_3 absorption edge, respectively. Colored areas in (c) and (h) correspond to the superconducting regions, where the maximum value of the vertical axis scales to be 15 K. [1] Yellow-colored areas and vertical dotted lines in (c), (d), (e), (h), (i), (j), and (k) correspond to the pressure around 2.5 GPa, where large changes in the electronic structure are observed, and the pressures of the structural transitions. [1]

with further increase of pressure. The increase of the intensity of the peak D at 2.5 GPa corresponds to the increase of the number of holes of the Bi 6s state and to the decrease of the carrier density in this case, which closely correlates to the rapid decrease of T_c. The energies of the absorption edge, the peak D, and the peak E increases at 2.5 GPa, rapidly decreases at 11 GPa, and gradually decreases above 20 GPa as shown in Figs. S2(h), S2(i), and S2(j), respectively. The intensity and energy of the peak F (6d e_g band) in Fig. S2(k) do not show a clear trend in the entire pressure range. The intensity of the peak D Fig. S2(i) does not change around the pressure 10 GPa of the first structural transition. However, its energy decreases rapidly. This possibly suggests the closing of the band gap and correlates with the increase of T_c above 11 GPa.

The pressure-induced change in the electronic structure occurs at the pressure of the first structural transition in Bi_2Se_3 and $Ag_{0.05}Bi_{1.95}Se_3$, and this structural transition induces superconductivity by strongly changing the electronic structure. But in $Sr_{0.19}Bi_2Se_3$, we did not observe the change in the electronic structure for both Se and Bi sites around 6 GPa where the superconductivity appears again with the structural transition. A possible scenario is the absence of the low-T_c region in the highly-doped $Sr_{0.19}Bi_2Se_3$ sample at the pressure range between 6–10 GPa, where superconductivity was observed in the low-doped samples. This remains as an unresolved problem.

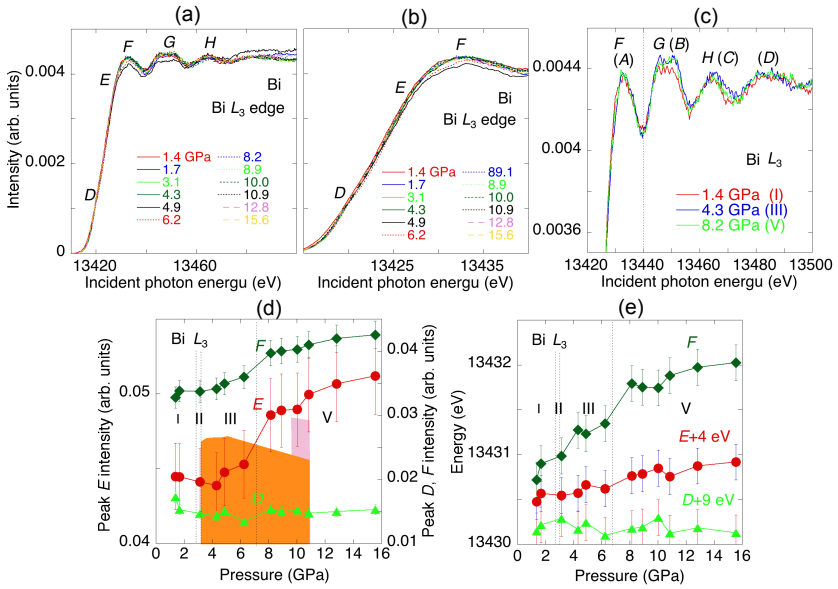

FIG. S3. (Color online). (a) Pressure dependence of the PFY-XAS spectra of Bi at the Bi-L_3 absorption edge. (b) Expanded views of the PFY-XAS spectra in (a) around the Bi-L_3 absorption edge. (c) Comparison of the PFY-XAS spectra of the phases II, III, and V. Note that the alphabetical symbols in the brackets are the notations used in the Ref. 7. (d) Pressure dependence of the intensity of the peaks D, E, and F of the PFY-XAS spectra. Colored areas in (c) corresponds to the superconducting regions, where the maximum value of the vertical axis scales to be 15 K. [9–11] (e) Pressure dependence of the energy of the peaks D, E, and F of the PFY-XAS spectra. Vertical dotted lines in (c) and (h) correspond to the pressures of the structural transitions. [12, 13]

C. Pressure dependence of the PFY-XAS spectra of Bismuth

Figures S3(a) and S3(b) show the pressure dependence of the PFY-XAS spectra of Bi at the Bi-L_3 absorption edge. In Bi, it is apparent that superconductivity is triggered by the structural phase transition from the phase II to III at 2.5 GPa, where the volume shows a step-like decrease. However, the pressure-induced change in the electronic structure is very small at this phase transition pressure. On the other hand, we observe an apparent change in the electronic structure around the third structural transition pressure of ∼7 GPa, where the phase transition from phase III to IV and a step-like decrease of the volume occurs. The electronic structure does not change much above 11 GPa, suggesting that superconductivity may persist above 11 GPa in Bi. Interestingly, the intensity of peaks E and F both increased around 7 GPa, indicating a decrease of the hybridization of Bi 6d bands. This behavior is different from the Bi_2Se_3-based compounds described above.

In Bi, normal XAS spectroscopy has been performed by Chen *et al.* [7] Pressure-induced changes in the electronic structure at each of the phases I, II, III, and V and good agreement with *ab initio* calculations were reported. Our present spectra show much higher resolution compared to the normal XAS spectra, but we did not observe such a clear difference of the spectra between the phases as shown in Fig. S3(c). Chen *et al.* found the emergence of peak E at 13442 eV in phase V and the disappearance of peak C (peak H in our spectra) or a merging of peaks C and D in phase III. Note that the alphabetical symbols in brackets are the notations used for our spectra. On the other hand, our spectra show an enhancement of the intensity of peak B (peak G in our spectra) in the phases III and V. The right shoulder intensity of peak C (peak H in our spectra) is also enhanced in phase III. The *ab initio* calculations by Chen *et al.* [7] showed that in Bi, the band gap closed at 2.7 GPa, and just above this pressure, superconductivity was observed. A further increase of the pressure caused an increase of the DOS at the Fermi level and the system gained a metallic character. Thus, in Bi the calculations also show, similar as in the Bi_2Se_3-based compounds under pressure, that superconductivity was observed with the closing of the band gap.

Bi has bcc structure in phase V. In Bi_2Te_3, a new absorption feature of the XANES spectrum around 13465 eV was observed in the bcc phase, which was considered to be caused by multiple scattering contributions in the medium range ordered structure. [8] However, in Bi no additional feature was observed in the bcc phase as shown in Fig. S3(c).

In Bi, a change in the electronic structure around 7 GPa at the phase transition from phase III to V was observed, while the change from phase II to III, where superconductivity emerges, was small.

In Bi the pressure-induced change in the electronic

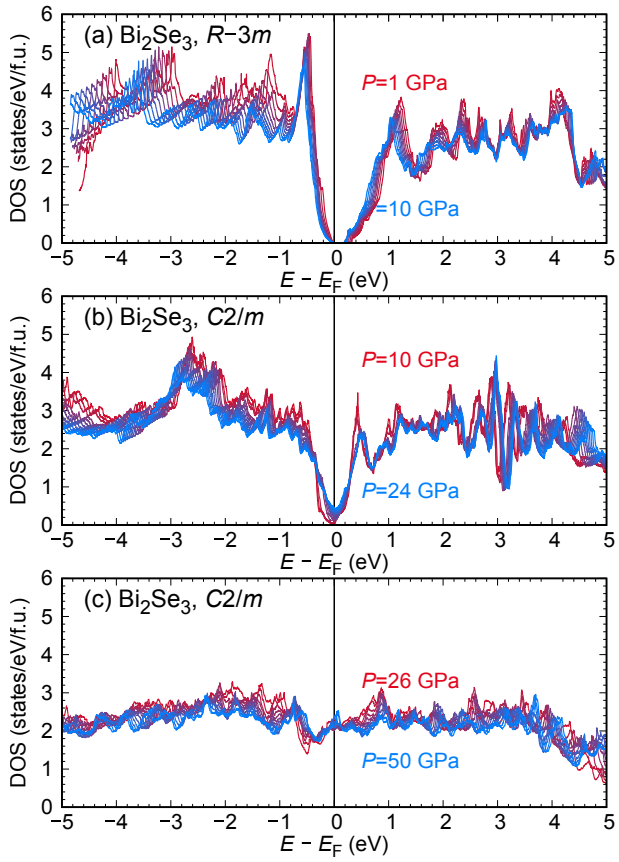

FIG. S4. (Color online). Pressure evolution of the total density of states in the phases (a) $R\bar{3}m$, (b) $C2/m$ (7-fold), and (c) $C2/m$ (bcc-like).

structure of Bi is not sensitive to the phase transitions from I to II and from II to III, while it is sensitive to that from III to V. In Bi_2Se_3 and $Ag_xBi_2Se_3$ the change in the electronic structures of both Bi and Se was observed at the transition from I to II, but it is not sensitive at the transition from II to III. The sensitivity of pressure-induced change in the electronic structure for the structural phase transition is different between Bi and Bi_2Se_3.

D. Pressure evolution of the density of states

Figures S4 and S5 show the pressure evolution of the total DOS and s partial DOS, respectively. In phase I, the total DOS shifts to higher binding energy, keeping the band gap at the Fermi level. In phase II, the total DOS below the Fermi level shifts to higher binding energy and that above the Fermi level shifts to lower binding energy. Meanwhile, the DOS near the Fermi level increases, indicating the pressure-induced broadening of the bands. In phase III, a similar trend as in phase II was observed, but the DOS at the Fermi level does not change much. Partial s DOS in Fig. S5 follows a similar trend as the total DOS in Fig. S4.

Figure S6 shows the total DOS and Bi $6p$ and Se $4p$ partial DOS at (a) 24.5 GPa (phase II) and (b) 25.5 GPa (phase IV) of Bi_2Se_3. The DOS at the Fermi level shows a jump between the phases II and IV. Between phase II and phase IV, Bi_2Se_3 experiences a 6% volume collapse. This leads to an increase of effective coordination number of Bi. The concomitant rearrangement of states leads to a partial occupation of previously empty Bi $6p$ and Se $4p$ states. These changes of the electronic structures cause the above jump the DOS at the Fermi level.

[1] Y. H. Zhou, X. L. Chen, R. R. Zhang, J. F. Shao, X. F. Wang, C. An, Y. Zhou, C. Y. Park, W. Tong, L. Pi, Z. R. Yang, C. J. Zhang, and Y. H. Zhang, Pressure-induced reemergence of superconductivity in topological insulator $Sr_{0.065}Bi_2Se_3$, Phys. Rev. B **93**, 144514 (2016).
[2] A. M. Nikitin, Y. Pan, Y. K. Huang, T. Naka, and

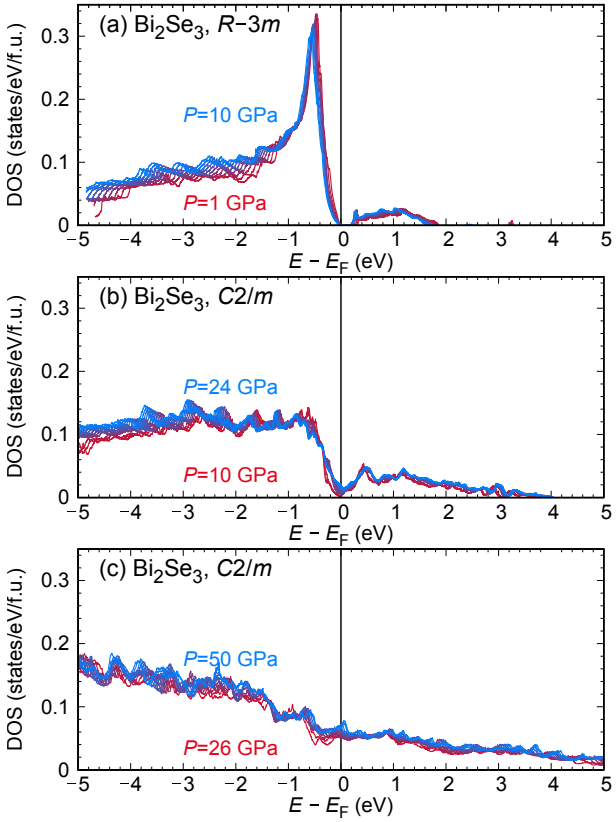

FIG. S5. (Color online). Pressure evolution of the s partial density of states at the phases of (a) $R\bar{3}m$, (b) $C2/m$ (7-fold), and (c) $C2/m$ (bcc-like).

A. de Visser, High-pressure study of the basal-plane anisotropy of the upper critical field of the topological superconductor $Sr_xBi_2Se_3$, Phys. Rev. B **94**, 144516 (2016).

[3] K. Manikandan, Shruti, P. Neha, G. Kalai Selvan, B. Wang, Y. Uwatoko, K. Ishigaki, R. Jha, V. P. S. Awana, and S. Arumugam, Possibility for conventional superconductivity in $Sr_{0.1}Bi_2Se_3$ from high-pressure transport studies, EPL **118**, 47008 (2017).

[4] Z. Liu, X. Yao, J. Shao, M. Zuo, L. Pi, S. Tan, C. Zhang, and Y. Zhang, Superconductivity with Topological Surface State in $Sr_xBi_2Se_3$, J. Am. Chem. Soc. **137**, 10512 (2015).

[5] Z. Li, M. Wang, D. Zhang, N. Feng, W. Jiang, C. Han, W. Chen, M. Ye, C. Gao, J. Jia, J. Li, S. Qiao, D. Qian, B. Xu, H. Tian, and B. Gao, Possible structural origin of superconductivity in Sr-doped Bi_2Se_3, Phys. Rev. Mater. **2**, 0142011 (2018).

[6] H. Leng, D. Cherian, Y. K. Huang, J.-C. Orain, A. Amato, and A. de Visser, Muon spin rotation study of the topological superconductor $Sr_xBi_2Se_3$, Phys. Rev. B **97**, 054503 (2018).

[7] H.-Y. Chen, S.-K. Xiang, X.-Z. Yan, L.-R. Zheng, Y. Zhang, S.-G. Liu, and Y. Bi, Phase transition of solid bismuth under high pressure, Chin. Phys. **25**, 108103 (2016).

[8] Z. Guo, H. Zhu, J. Dong, Q. Jia, Y. Gong, Y. Wang, H. Li, P. An, D. Yang, Y. Zhao, H. Xing, X. Li, and D. Chen, Local structural changes during the disordered substitutional alloy transition in Bi_2Te_3 by high-pressure XAFS, J. Appl. Phys. **124**, 065901 (2018).

[9] M. A. Il'ina and E. S. Itskevich, New superconducting modifications of Bi, JETP Lett. **11**, 218 (1972).

[10] M. A. Il'ina, Superconducting properties of the bismuth-antimony system at high pressures, Sov. Phys. Solid State **18**, 600 (1976).

[11] Y. Li, E. Wang, X. Zhu, and H.-H. Wen, Pressure-induced superconductivity in Bi single crystals, Phys. Rev. B **95**, 024510 (2017).

[12] M. I. McMahon, O. Degtyareva, and R. J. Nelmes Ba-IV-Type Incommensurate Crystal Structure in Group-V Metals, Phys. Rev. Lett. **85**, 4896 (2000).

[13] C. G. Homan, Phase diagram of Bi up to 140 kbars, J. Phys. Chem. Solids **36**, 1249 (1975).

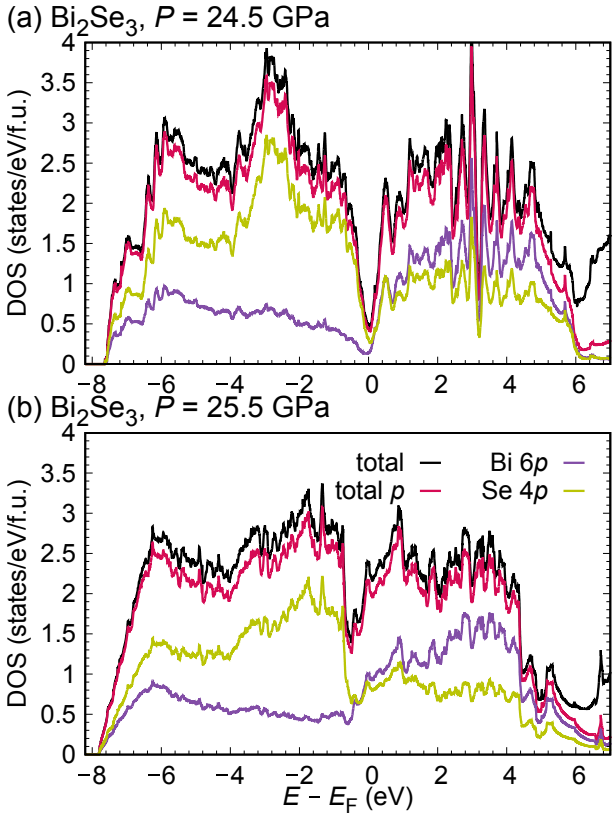

FIG. S6. (Color online). Total DOS and Bi 6p and Se 4p partial DOS at (a) 24.5 GPa (phase II) and 25.5 GPa (phase (IV) of Bi_2Se_3.